Journal of Photochemistry and Photobiology A: Chemistry 221 (2011) 38–46

Contents lists available at ScienceDirect

Journal of Photochemistry and Photobiology A: Chemistry

journal homepage: www.elsevier.com/locate/jphotochem

Synthesis and photophysical behaviour of tantalum and titanium phthalocyanines in the presence of gold nanoparticles: Photocatalysis towards the oxidation of cyclohexene

Vongani P. Chauke[a], Yasin Arslanoglu[a,b], Tebello Nyokong[a,*]

[a] Department of Chemistry, Rhodes University, Grahamstown 6140, South Africa
[b] Department of Chemistry, Istanbul Technical University, 34469 Maslak, Istanbul, Turkey

ARTICLE INFO

Article history:
Received 2 January 2011
Received in revised form 12 April 2011
Accepted 17 April 2011
Available online 22 April 2011

Keywords:
Tantalum
Titanium
Phthalocyanines
Gold nanoparticles
Singlet oxygen quantum yield
Photocatalysis
Photodegradation
Triplet quantum yields
Triplet lifetimes
Cyclohexene

ABSTRACT

We report on the synthesis of 2,(3)- (peripheral) and 1,(4)- (non-peripheral) (2-mercaptopyridine)phthalocyanine complexes of titanium (IV) oxide (**5** and **6** respectively), and tantalum (III) hydroxide (**7**, peripheral only), their photochemical and photophysical parameters and the photocatalytic oxidation of cyclohexene in the presence of gold nanoparticles (AuNPs). The singlet oxygen quantum yield values increased in the presence of AuNPs, for complexes **5** and **6**. The percentage conversion values for cyclohexene using **5**, **6** and **7** were 27%, 20% and 14%, respectively. These values increased considerably in the presence of AuNPs, except complex for **7**. The products obtained include cyclohexene oxide, 2-cyclohexen-1-ol, 2-cyclohexene-1-one and 1,2-cyclohexanediol. Low values of singlet oxygen quantum yields favour the formation of 1,2-cyclohexanediol.

1. Introduction

Phthalocyanines (Pc) are synthetic macrocyclic compounds that have similar properties to the naturally occurring porphyrins [1]. They comprise of different characteristics depending on the type of substituents, position of substitution and metal centre. Of interest, particularly to this work (photocatalysis), are their light absorption characteristics [2]. Pcs find many applications in light driven processes such as photodynamic therapy (PDT) [3], solar cells technology [4] and photocatalysis [5,6]. These applications are possible due to the Pcs' ability to produce singlet oxygen or various reactive oxygen species such as superoxide radicals [7,8]. Photocatalysis using metallophthalocyanines (MPcs) [7,9–13] has been reported to involve mainly singlet oxygen species.

Metal nanoparticles, particularly gold nanoparticles (AuNPs) have been used in many different fields that include catalysis [14], photocurrent generation [15] and photocatalysis [16]. This is owed to their tunable size and shape which result in their tunable optical properties [17]. AuNPs absorb visible light due to the surface plasmon resonance (SPR) effects [18]; which is a collective oscillation of conduction electrons in the nanoparticles, which resonate with the electromagnetic field of the incident light [19].

In this work, we report on the photooxidation of cyclohexene using the newly synthesized TiPc (**5** and **6**) and TaPc (**7**) complexes (Scheme 1) in the presence of AuNPs. Not much attention has been paid to the photooxidation of alkenes and alkanes using MPcs in the presence of AuNPs. We have recently reported [20] on the photocatalytic oxidation of cyclohexene using TaPc complexes non-peripherally substituted with alkyl chains, in the presence of AuNPs where the TaPc complexes were irradiated at the Q band region and with white light. The major drawback with the latter was drastic photobleaching of the TaPc complexes. We therefore concentrated on the irradiations at the Q band of the MPcs in the current work. The choice of the central metals is due to their size which allows for the generation of large singlet oxygen quantum yields due to enhanced intersystem crossing [20,21]. The choice

* Corresponding author. Tel.: +27 46 6038260; fax: +27 46 6225109.
E-mail address: t.nyokong@ru.ac.za (T. Nyokong).

1010-6030/$ – see front matter © 2011 Elsevier B.V. All rights reserved.
doi:10.1016/j.jphotochem.2011.04.020

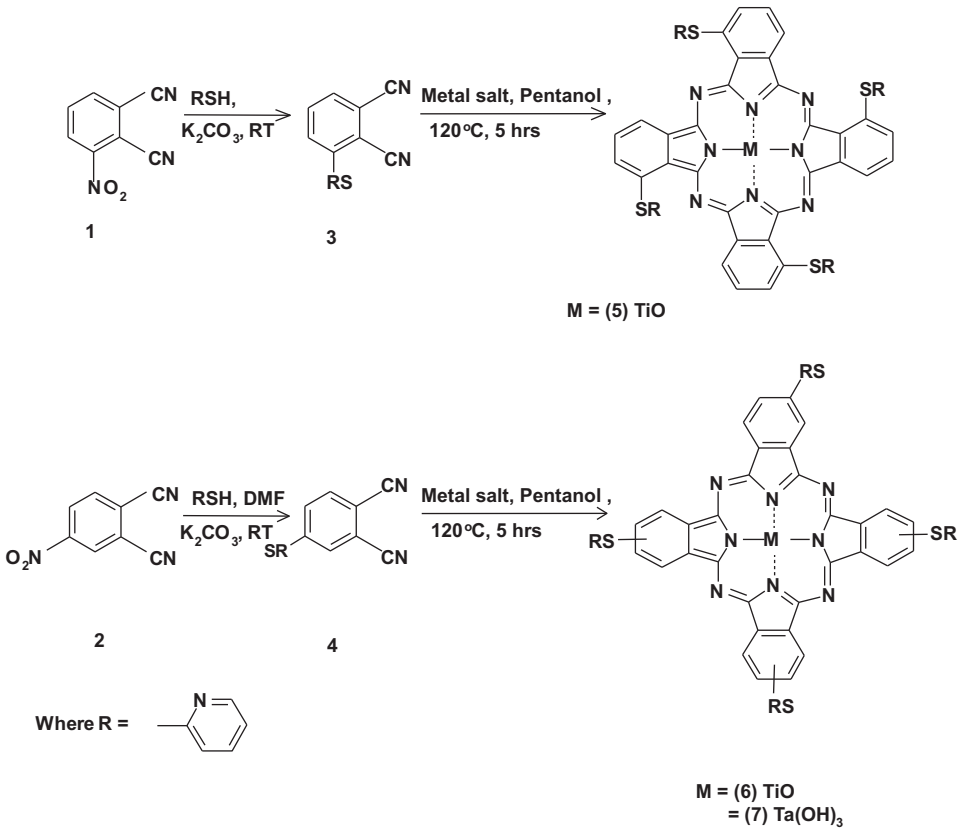

Scheme 1. Synthetic route for complexes **5**–**7**.

of the bulky mercaptopyridine substituents is expected to prevent aggregation. In addition, the presence of sulfur bridges allows for red shifting of spectra in phthalocyanines [22]. The effect of the central metal as well as the point of substitution (peripheral versus non-peripheral) will be explored. We also studied the photostability of these complexes as well as their efficiency as photosensitizers (singlet oxygen, and triplet quantum yields and lifetimes).

The importance of alkenes and alkanes oxidation has been reiterated and explored quite extensively due to the usefulness of the oxidation products to industrial processes as well as fine chemical syntheses [6]. The oxidation products of alkenes include alcohols, ketones and aldehydes.

2. Experimental

2.1. Materials

Zinc(II) phthalocyanine (ZnPc), 1,3-diphenylisobenzofuran (DPBF), cyclohexene, cyclohexene oxide, 2-cyclohexene-1-ol, cyclohexene-1-one, 1,2-cyclohexanediol, 1,4-diazobicyclo-octane (DABCO), benzoquinone, toluene, 1-pentanol, and titanium (IV) butoxide, tantalum (V) butoxide and 1,8-diazabicyclo[5,4,0]undec-7-ene (DBU) were from Sigma–Aldrich. Tetraoctylammonium bromide (TOABr) (98%), gold(III) chloride trihydrate and sodium borohydride ($NaBH_4$) (96%) were purchased from Fluka. Gold nanoparticles were synthesized as reported before [23,24].

Potassium carbonate, ethanol, methanol, tetrahydrofuran (THF), chloroform, deuterated chloroform ($CDCl_3$) acetone, and dimethylformamide (DMF), were obtained from Merck. Ultra pure water was obtained from a Milli-Q Water System (Millipore Corp, Bedford, MA, USA). Column chromatography was performed on silica gel 60 (0.04–0.063 mm) and preparative thin layer chromatography was performed on silica gel 60 P F_{254}.

2.2. Equipment

A Shimadzu UV-2550 spectrophotometer was employed for the collection of UV–Vis spectra. Infra-red spectra (KBr pellets) were recorded on Perkin Elmer Spectrum 2000 FT-IR Spectrometer and ^{1}H nuclear magnetic resonance signals on a Bruker EMX 400 NMR spectrometer.

A laser flash photolysis system was used for the determination of triplet state lifetimes and quantum yields. The excitation pulse was produced by a Qunta-Ray Nd:YAG laser (1.5 J/9 ns), pumping a Lambda Physik FL 3002 dye laser (Pyridin 1 in methanol). The analysing beam source was from a Thermo Oriel 66902 xenon arc lamp, and a Kratos Lis Projekte MLIS-X3 photomultiplier tube was used as a detector. Signals were recorded with a two-channel, 300 MHz digital real time oscilloscope (Tektronix TDS 3032C); the kinetic curves were averaged over 256 laser pulse. Triplet lifetimes were determined by exponential fitting of the kinetic curves using OriginPro 7.5 software.

Elemental analyses were carried out on a Vario EL III MicroCube CHNS Analyzer. Mass spectral data were collected with a Bruker AutoFLEX III Smartbeam TOF/TOF Mass spectrometer. The instrument was operated in positive ion mode using an m/z range of 400–3000. The voltage of the ion sources was set at 19 and 16.7 kV for ion sources 1 and 2 respectively, while the lens was set at 8.50 kV. The reflector 1 and 2 voltages were set at 21 and 9.7 kV respectively. The spectra were acquired using dithranol as the MALDI matrix, using a 354 nm N_2 laser.

Transmission electron microscope (TEM) images were obtained using a JEOL JEM 1210 transmission electron microscope at 100 kV accelerating voltage. A few drops of the solutions of the samples were placed on carbon coated 300 mesh grids and were left to dry for about 30 s. X-ray powder diffraction patterns were recorded on a Bruker D8, Discover equipped with a proportional counter, using

Cu Kα radiation (λ = 1.5405 Å, nickel filter). Data were collected in the range from $2\theta = 5^\circ$ to 60°, scanning at $1^\circ\,min^{-1}$ with a filter time-constant of 2.5 s per step and a slit width of 6.0 mm. Samples were placed on a silicon wafer slide. The X-ray diffraction data were treated using Eva (evaluation curve fitting) software. Baseline correction was performed on each diffraction.

2.3. Photochemical methods

General Electric Quartz line lamp (300 W) was employed for the determination of photodegradation and singlet oxygen quantum yields, and for the phototransformation of cyclohexene. A 600 nm glass cut off filter (Schott) and a water filter were used to filter off ultraviolet and infrared radiations respectively. An interference filter (Intor, 740 nm with a band width of 40 nm) was additionally placed in the light path before the sample, hence ensuring excitation at the Q band only (700–780 nm). Light intensities were measured with a POWER MAX 5100 (Molelectron detector incorporated) power meter.

The products for the phototransformation of cyclohexene were analyzed using an Agilent HP 5890 gas chromatograph (GC), fitted with a flame ionization detector (FID), using a DB-5MS column (0.25 m length, 0.2 mm internal diameter, 0.25 μm film thickness). The GC parameters were as follows: the initial oven temperature was at 50 °C, maximum oven temperature was 280 °C, equilibration time was 0.15 min, initial ramp rate was 10 °C/min at 180 °C for 2 min, the second was 10 °C/min at 280 °C for 2 min and total run time was 27 min.

Reactions were carried out under homogeneous conditions in toluene. The reaction mixture consisted of complexes **5**–**7** or **5**–**7**-AuNP mixed with known concentration of the cyclohexene. The reaction mixture was contained in a reaction vessel maintained at room temperature under constant stirring, and photolysed using the set-up described above. The reaction was then monitored by taking samples of the solution and recording UV spectra or gas chromatographs. Light intensity for these studies was 1.4×10^{17} photons $s^{-1}\,cm^{-2}$.

2.4. Photochemical and photophysical parameters

2.4.1. Singlet oxygen quantum yields

Quantum yields of singlet oxygen photogeneration by TaPc or TiPc derivatives in toluene were determined in air (no oxygen bubbled) using the relative method with ZnPc as reference and DPBF as chemical quencher for singlet oxygen, using Eq. (1):

$$\Phi_\Delta = \Phi_\Delta^{Std} \cdot \frac{R_{DPBF} I_{abs}^{Std}}{R_{DPBF}^{Std} I_{abs}} \quad (1)$$

where Φ_Δ^{Std} is the singlet oxygen quantum yield for the standard, ZnPc ($\Phi_\Delta = 0.58$ in toluene [25]), R_{DPBF} and R_{DPBF}^{Std} are the DPBF photodegradation rates in the presence of a sensitizer under investigation and the standard respectively. I_{abs} and I_{abs}^{Std} are the rates of light absorption by the sensitizer and standard, respectively.

To avoid chain reactions induced by DPBF in the presence of singlet oxygen [26], the concentration of DPBF was lowered to $\sim 3 \times 10^{-5}$ mol dm^{-3}. Solutions of sensitizer (absorbance = 0.2 at the irradiation wavelength) containing DPBF were prepared in the dark and irradiated in the Q band region using the setup described above. DPBF degradation at 415 nm was monitored. The light intensity for singlet oxygen studies was 5×10^{15} photons $s^{-1}\,cm^{-2}$.

2.4.2. Photodegradation quantum yields

For determination of photodegradation quantum yields of the TaPc or TiPc derivatives, the usual Eq. (2) [26] was employed:

$$\Phi_P = \frac{(C_0 - C_t) V N_A}{I_{abs} S t} \quad (2)$$

where C_0 and C_t (mol dm^{-3}) are the concentrations of TiPc and TaPc complexes (**5**–**7**) before and after irradiation respectively; V is the reaction volume; S, the irradiated cell area (2.0 cm^2); t, the irradiation time (s); N_A, the Avogadro's number and I_{abs}, the overlap integral of the radiation source intensity and the absorption of the Pc (the action spectrum) in the region of the interference filter transmittance. For experiments where the TiPc and TaPc complexes were irradiated in the presence of AuNPs, any absorption of the latter was subtracted from the DPBF absorption to avoid any errors.

2.4.3. Triplet quantum yields and lifetimes

The solutions for triplet quantum yields and lifetimes were introduced into a 1 cm pathlength UV/visible spectrophotometric cell, deaerated using argon and irradiated at the Q band maxima. Triplet state quantum yields (Φ_T) of the TiPc (**5** and **6**) and TaPc (**7**) complexes and their AuNPs derivates were determined by the triplet absorption method. A comparative method [27] using zinc phthalocyanine as a standard was employed for the calculations, Eq. (3):

$$\Phi_T = \Phi_T^{Std} \cdot \frac{\Delta A_T . \varepsilon_T^{Std}}{\Delta A_T^{Std} . \varepsilon_T} \quad (3)$$

where ΔA_T and ΔA_T^{Std} are the changes in the triplet state absorbances of the TiPc or TaPc derivatives and the standard, respectively. ε_T and ε_T^{Std} are the triplet state molar extinction coefficients for the TiPc or TaPc derivatives and the standard, respectively. Φ_T^{Std} is the triplet quantum yield for the standard, ZnPc ($\Phi_T = 0.65$ in toluene [28]). ε_T and ε_T^{Std} were determined from the molar extinction coefficients of the respective ground singlet state (ε_S and ε_S^{Std}), the changes in absorbances of the ground singlet states (ΔA_S and ΔA_S^{Std}) and changes in the triplet state absorptions, (ΔA_T and ΔA_T^{Std}) according to Eqs. (4a) and (4b):

$$\varepsilon_T = \varepsilon_S \frac{\Delta A_T}{\Delta A_S} \quad (4a)$$

$$\varepsilon_T^{Std} = \varepsilon_S^{Std} \frac{\Delta A_T^{Std}}{\Delta A_S^{Std}} \quad (4b)$$

2.5. Synthesis of phthalocyanine derivatives

The synthesis of the mercaptopyridine phthalonitrile (**3** and **4**) has been reported [29].

2.5.1. 1,(4)-(2-Mercaptopyridine)phthalocyaninato titanium (IV) oxide (**5**), Scheme 1

Under a stream of nitrogen, a mixture of titanium butoxide (0.25 g, 1.5 mmol), 3-(2-mercaptopyridine)phthalonitrile (**3**) (0.5 g, 2.1 mmol), DBU (1.66 mL, 12 mmol) and 1-pentanol (10 mL) was stirred at 160 °C for 5 h. After cooling, methanol was added to the reaction solution. The resulting precipitate was filtered and washed twice methanol. The mixture was cooled and column chromatography over silica was done with $CHCl_3$ as eluent. Yield: 0.38 g (64%). UV/Vis (toluene): λ_{max} (nm) (log ε) 335(4.45), 642(4.46), 720(5.12). IR (KBr): ν_{max}/cm^{-1}; 3058 (Ar-H), 1558 (C=C), 1523, 1452, 1345, 1201, 1109, 1093 (C–S–C), 898 (Ti=O). ^{1}H NMR ($CDCl_3$): δ, ppm: 8.90–9.35 (m, 5H, Pc-H), 8.45–8.89 (m, 7H, Pc-H), 7.75–8.25 (m, 8H, Pyridyl-H), 7.43-7.68 (m, 8H, Pyridyl-H), Calc. for $C_{52}H_{28}N_{12}S_4OTi$:

C 61.64; H 2.78; N 16.59; S 12.65; found: C 61.07, H 2.90, N 15.78, S 12.51. MALDI-TOF MS *m/z*: Calcd: 1013 amu. Found: $[M-H]^+$ 1012 amu.

2.5.2. 2,(3)-(2-Mercaptopyridine)phthalocyaninato titanium (IV) oxide (**6**), Scheme 1

The synthesis of **6** was as outlined for **5** except **4** was employed instead of **3**. The amounts of reagents employed were: **4** (0.25 g, 1.05 mmol), titanium butoxide (0.66 g, 5.26 mmol), DBU (1.66 mL, 12 mmol) and 1-pentanol (10 mL). Yield: 0.32 g (54%). UV/Vis (toluene): λ_{max} (nm) ($\log\varepsilon$) 335(5.17), 635(4.80), 701(5.58). IR (KBr): ν_{max}/cm^{-1}; 3063 (Ar-H), 1560 (C=C), 1523, 1452, 1345, 1201, 1109, 1095 (C–S–C), 900 (Ti=O). ^{1}H NMR ($CDCl_3$): δ, ppm: 8.50–9.25 (m, 8H, Pc-H), 7.75–8.49 (m, 4H, Pc-H), 6.75–7.40 (m, 16H, Pyridyl-H), Calc. for $C_{52}H_{28}N_{12}S_4OTi$: C 61.64; H 2.78; N 16.59; S 12.65; found: C 62.09, H 3.01, N 15.96, S 12.49. MALDI-TOF MS *m/z*: Calcd: 1013 amu. Found: $[M-H]^+$ 1012 amu.

2.5.3. 2,(3)-(2-Mercaptopyridine)phthalocyaninato tantalum (V) hydroxide (**7**), Scheme 1

The synthesis of **7** was as outlined for **5** except **4** instead of **3**, and tantalum butoxide instead of titanium butoxide were used. The amounts of reagents employed were: **4** (0.25 g, 1.05 mmol), tantalum butoxide (0.66 g, 1.21 mmol), DBU (1.66 mL, 12 mmol) and 1-pentanol (10 mL). Yield: 0.25 g (42%). UV/Vis (toluene): λ_{max} (nm) ($\log\varepsilon$) 335(4.59), 620(4.15), 688(5.74), 710(5.79). IR (KBr): ν_{max}/cm^{-1}; 3063 (Ar-H), 1560 (C=C), 1523, 1452, 1345, 1201, 1307, 1285, 1201, 1109, 1095 (C–S–C), 910, (Ta–O). ^{1}H NMR ($CDCl_3$): δ, ppm: 8.32–9.33 (m, 8H, P-H), 7.71–8.50 (m, 4H, Pc-H), 6.70–7.30 (m, 16H, Pyridyl-H), Calc. for $C_{52}H_{31}N_{12}S_4O_4Ta$: C 52.16; H 2.61; N 14.04; S 10.71; found: C 52.09, H 3.04, N 14.04, S 10.45. MALDI-TOF MS *m/z*: Calcd: 1197 amu. Found: [M–Ta] 965 amu.

2.6. Synthesis of AuNP and its conjugates of with complexes **5**–**7**

The synthesis of gold nanoparticles (using phase transfer agent TOABr as a protecting ligand) was achieved following the method described by Brust et al. [23] and Kotiaho et al. [24] with slight modifications. Briefly gold (III) chloride trihydrate solution (25 mmol L^{-1}, 4 mL) was vigorously stirred with a solution of TOABr (85 mmol L^{-1}, 6 mL) in toluene until all the gold chloride was transferred to the organic phase, as judged by the change of colour from orange to red [23,24]. An aqueous solution of a reducing agent $NaBH_4$ (3.6×10^{-2} mol L^{-1}) was then added drop-wise over a period of 10 min. The mixture was then stirred vigorously for 30 min. The organic phase was separated and washed with water.

X-ray diffraction (XRD) was used to determine the size of the particles (as reported before [20]) using the Debye–Scherrer equation (5):

$$d\,(\text{Å}) = \frac{k\lambda}{\beta\cos\theta} \tag{5}$$

where k is an empirical constant equal to 0.9, λ is the wavelength of the X-ray source, (1.5405 Å), β is the full width at half maximum of the diffraction peak, and θ is the angular position of the peak. The average size for the AuNPs was then worked out to be 10.1 nm, using the peak that fits the structure database reflection for gold.

Solid complexes of conjugates of **5**–**7** with AuNPs were synthesized by mixing the two, allowing time (~28–30 h) for the MPcs to react with the gold nanoparticles. The solvent (toluene) was then evaporated. The uncoordinated TiPc and TaPc derivatives were removed using a size-exclusion column (bio-beads) as reported before [30].

3. Results and discussion

3.1. Synthesis and characterization

Scheme 1 gives the synthetic pathways for the TiPc (**5** and **6**) and TaPc (**7**) complexes discussed in this work. Complexes **3** and **4** were treated with 1-pentanol, the corresponding metal salts {titanium (IV) butoxide, or tantalum (V) butoxide} and DBU as the catalyst to afford TiPc (**5** and **6**) and TaPc (**7**) complexes (Scheme 1). Column and preparative thin layer chromatography with silica gel were employed to obtain the pure products from the reaction mixtures. The synthesised complexes (**5**–**7**) are soluble in organic solvents such as dichloromethane, chloroform, chloronaphthalene, dimethlyformamide (DMF) and dimethlysulfoxide (DMSO). The new compounds were characterized by UV–Vis, IR and NMR spectroscopies, and elemental analysis. The analyses are consistent with the predicted structures as shown in Section 2.

The new complexes were found to be pure by ^{1}H NMR with all the substituents and ring protons observed in their respective regions. The metal salts employed for synthesis of the MPc complexes were titanium butoxide and tantalum butoxide, however the axial ligands obtained are oxo and hydroxide as a result of the purification process and the MPcs.

The ground state electronic absorption spectra the synthesized complexes are shown in Fig. 1. Complex **5** {with susbtituents on the α (non-peripheral) position} shows broad and red-shifted spectrum Fig. 1a, relative to complex **6** which is β- (peripheral) substituted. This red shift is typical for MPc complexes substituted at the non-peripheral positions [31].

The broadening in the spectra of **5** could be a result of aggregation or loss of symmetry due to the presence of bulky groups at the non-peripheral positions. Aggregation at the concentrations in Fig. 1 was ruled out since Beer's law was obeyed for concentrations ranging from 2.85×10^{-6} to 1.34×10^{-5} mol dm^{-3}. The most likely reason for the broadening is the loss of symmetry. It has been reported that deformation of the Pc ring occurs when bulky substituents such as methoxyphenyl groups are located at non-peripheral positions [32]. The loss of symmetry is more pronounced for TaPc derivative (Fig. 1b) as judged by the split Q band, even though this complex is substituted at peripheral positions. Fig. 1c does not show a faster decrease in the blue shifted peak for **7** relative to the low energy, which would be expected if H aggregates were present. Addition of a surfactant, Triton X 100 to **7** did not result in any changes in spectra which could be attributed to monomerization. The larger split in the Q band for **7** could be due to the large size of the Ta central metal which lies more out of the plane of the ring when compared to the other central metals.

Fig. 2 shows the transmission electron microscopy (TEM) images of AuNPs (Fig. 2a) and MPc-AuNPs (Fig. 2b, using TaPc (**7**) as an example). Fig. 2a shows a spherical nature of the AuNPs and Fig. 2b, the TaPc appears to be around the gold nanoparticles, as evidenced by the dark areas on the AuNP. It is possible that the MPc complexes are simply adsorbed onto the AuNPs. As reported before [20], we found no evidence (using Raman spectroscopy) of an Au–S bond which would be the case if the stabilizer (citrate) on AuNPs were replaced by TaPc resulting in the alkylthio groups attaching to Au.

3.2. Triplet quantum yields (Φ_T) and lifetimes (τ_T)

Triplet quantum yield (Φ_T) is a measure of the fraction of absorbing molecules that undergo intersystem crossing to the meta-stable triplet excited state. The competence of phthalocyanines as photocatalysts or photosensitisers depends on their high triplet quantum yields and lifetimes. A typical triplet decay curve for complex **5** is shown in Fig. 3. The triplet quantum yield (Φ_T) values were higher for complexes **5** and **6** (0.67 and 0.62, respectively, Table 1) com-

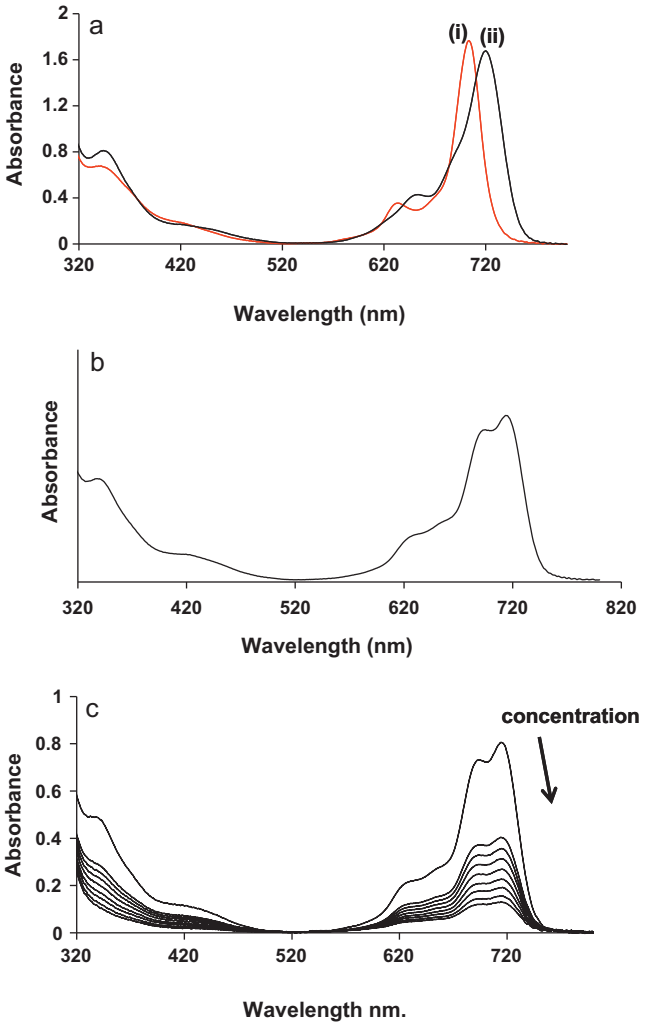

Fig. 1. UV–Vis spectra of complexes (a) **6** (i, 5×10^{-6} mol L^{-1}) and **5** (ii, 1×10^{-5} mol L^{-1}) and (b) and **7** (5×10^{-6} mol L^{-1}) in toluene. (c) The spectral changes for **7** in the concentration range = 2.12×10^{-6}–1.34×10^{-5} mol L^{-1}.

pared to the TaPc complex (**7**) with a value of 0.28. The low value of Φ_T for TaPc (**7**) could be a result of low symmetry discussed above. It has been reported that loss of symmetry leads to efficient radiationless deactivation of the lowest excited states of free-base porphyrin [33], this could be the case for TaPc (**7**) resulting in low Φ_T value. AuNPs improved the triplet quantum yields for **5** and **6** and this is due to enhanced spin–orbit coupling through heavy atom effect of gold, Table 1. The presence of the bromide atoms on TOABr (the AuNPs protecting ligand) also increases the energy transfer to the triplet state of TiPc complexes in the presence of AuNPs through enhanced spin-orbit coupling by heavy atom effect. For complex **7**, there is however no increase in Φ_T value. The triplet lifetime values (Table 1) are lower than is typical of phthalocyanines [25], due to the heavy atom effect. These values decrease further in the presence of AuNPs, again due to the heavy atom effect.

Table 1
Singlet oxygen and photobleaching quantum yields and rate constants for complexes **1**a and **1**b in the absence and presence of AuNPs in toluene.

MPc	Φ_T	τ_T (μs)	$\Phi_\Delta \pm 0.02$	$\Phi_P/10^5$
5	0.67	79	0.63	2.29
6	0.62	82	0.54	5.66
7	0.28	49	0.41	0.52
5-AuNPs	0.70	34	0.72	3.73
6-AuNPs	0.74	27	0.67	2.18
7-AuNPs	0.26	20	0.23	0.18

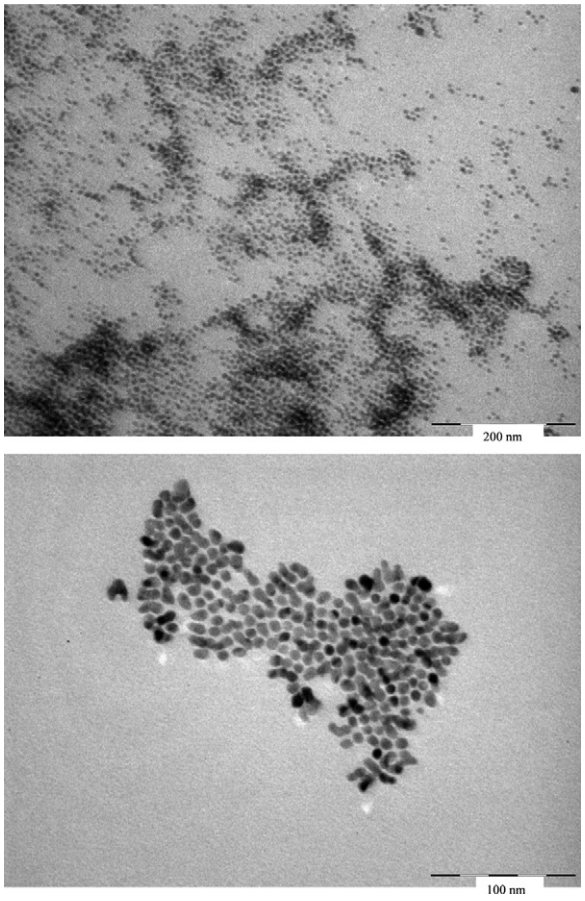

Fig. 2. TEM images of (a) AuNPs and (b) AuNPs modified with complex **7**.

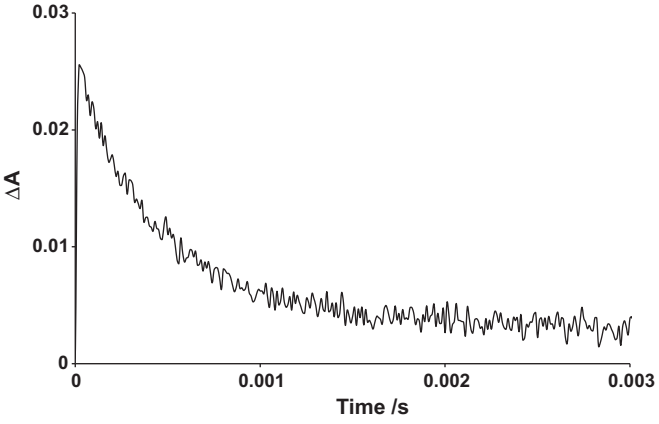

Fig. 3. Triplet decay curve for **5** in toluene.

3.3. Singlet oxygen quantum yield (Φ_Δ) of the TaPc derivatives

Singlet oxygen quantum yields are an evaluation of a phthalocyanine's ability to produce singlet oxygen. Singlet oxygen plays a significant role in photocatalytic oxidation reactions [26]. Singlet oxygen quantum yield (Φ_Δ) values (Table 1) were determined using DPBF as the singlet oxygen quencher in toluene. Complexes, **5**–**7** showed relatively good singlet quantum yield values that

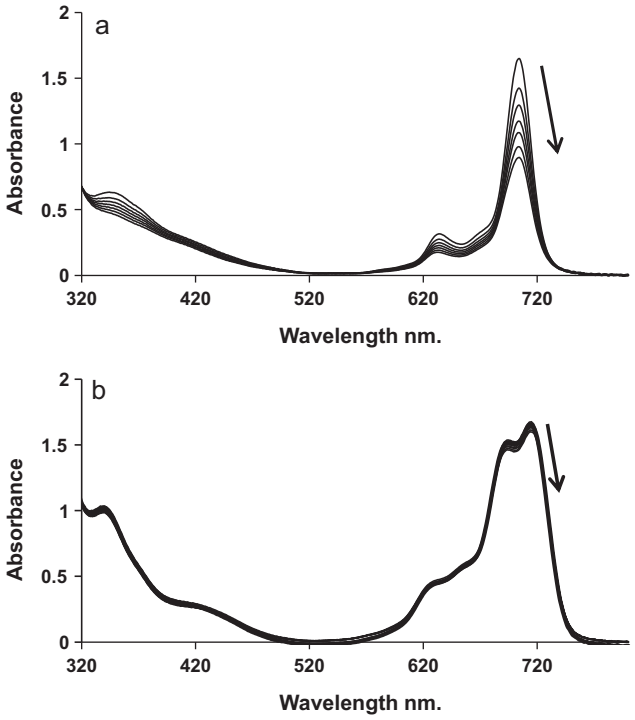

Fig. 4. Photodegradation spectra of complex (a) **6** and **7** in toluene. [**5**] = 3.4×10^{-5} mol L^{-1} and [**7**] = 2.1×10^{-5} mol L^{-1}.

ranged from 0.41 to 0.63, with TaPc complex exhibiting the lowest value of 0.41, due to the low value of triplet quantum yield. On introducing AuNPs to the TiPc and TaPc complexes, a drastic increase of the Φ_Δ values for the TiPc complexes (**5** and **6**) was observed, Table 1. This is attributed the heavy atom effect by the gold nanoparticles, which give large Φ_T values hence correspondingly large Φ_Δ values. The Φ_Δ value for **5**-AuNP was almost the same (within experimental error) as the Φ_T value showing efficient energy transfer from the triplet state of the phthalocyanine (complex **5**) to the ground state oxygen. The Φ_Δ value for **7**-AuNP decreased, corresponding to the low Φ_T value.

3.4. Photodegradation quantum yields (Φ_P) of the phthalocyanine derivatives

In order to determine the number of MPc molecules degraded per photon of light absorbed, the photodegradation quantum yield values were calculated. A photochemical process whereby the conjugated chromophore of the phthalocyanine ring gets degraded into smaller molecular fragments is defined as photodegradation. This process is driven by singlet oxygen in the presence of visible light to afford the photo-oxidation product, phthalamide, as suggested by Schnurpfeil et al. [26]. Photostability of MPc complexes is important for their application as photocatalysts (photosensitizers). The photodegradation stabilities were determined in toluene by monitoring the spectra of the complexes with increasing time, during photolysis, Fig. 4a and b. The MPc complexes are degraded by singlet oxygen generated by them. Generally, all the complexes in this work were very stable, with Φ_P values ranging from 5.66×10^{-5} to 1.80×10^{-6}, Table 1. Typical values for unstable phthalocyanines are of the order of 10^{-3} [34]. The TaPc derivative (in particular) was very stable, shown in Fig. 4b and Table 1. The stability of complex **7** correlates well with its low singlet oxygen production, since singlet oxygen is responsible for the degradation of MPcs.

Table 2
Percentage conversion of cyclohexene by complexes 5-7 and their conjugates with AuNPs in toluene. Photolysis time = 180 min.

MPc	% conversion
5	27
6	20
7	14
5-AuNPs	40
6-AuNPs	38
7-AuNPs	12

$$\%\,\text{conversion} = \frac{(1-\text{cylohexene}_{\text{initial}})-(1-\text{cyclohexene}_{\text{remaining}})}{1-\text{cyclohexene}_{\text{initial}}} \times 100.$$

3.5. Photocatalytic oxidation of cyclohexene

The products for photooxidation of cyclohexene obtained in this work were confirmed by the spiking the photocatalysed samples with the respective standards. Control experiments were performed where cyclohexene was photo-oxidized in the absence of MPcs or MPc-AuNP conjugates. The results for the control experiments showed negligible formation of the products. Similarly, in the absence of light but in the presence of TiPc and TaPc derivatives (with or without AuNPs), no products were formed.

The main products obtained for photocatalysed oxidation of cyclohexene (confirmed by spiking) are: cyclohexene oxide, 2-cyclohexen-1-ol, 2-cyclohexene-1-one and 1,2-cyclohexanediol. These products were also reported for TaPc derivatives containing long chain substitituents [20]. Some of the reported [9,10] photo-transformation products for cyclohexene include cyclohexene oxide, cyclohexenol and cyclohexenone. Photooxidation of cyclohexene using Pd, Al and Zn sulfonated phthalocyanines gave mainly cyclohexene hydroperoxide with cyclohexenol and cyclohexenone as minor products [9]. Using chemical oxidants {*tert*-butylhydroperoxide (TBHP) or chloroperoxybenzoic acid (CPBA)} and very long reaction times (four weeks), adipic acid was obtained using iron(II) polychlorophthalocyanine ($FePcCl_{16}$), iron(II) phthalocyanine (FePc) or cobalt(II) phthalocyanine (CoPc) as catalysts, in addition to cyclohexene oxide, cyclohexenol and cyclohexenone [10]. In this work the same products (cyclohexene oxide, cyclohexenol and cyclohexenone) were formed as reported in literature [9,10], but in addition cyclohexanediol was formed instead of cyclohexene hydroperoxide reported for photooxidation using sulfonated phthalocyanines. The products formed in phototransformation of cyclohexene are strongly influenced by the nature of the solvent and the nature of photosensitiser. The formation of cyclohexene hydroperoxide was observed when a CH_3CN:Water solvent mixture was employed, while in the current study, the reactions were performed in toluene.

The percentage conversion values of cyclohexene are summarized in Table 2 for complexes **5**–**7** and their AuNPs conjugates under Q band irradiation for 180 min. The percentage conversion values were noticeably increased on AuNPs conjugation (except for complex **7**). The values for **5**, **6** and **7** were 27%, 20% and 14%, respectively. In the presence of AuNPs, these values increased significantly except for TaPc whose value decreased to 12%, corresponding to decrease in the Φ_Δ value. On the other hand, the drastic increase in percentage conversion values for AuNPs conjugated TiPc complexes (**5**-AuNPs and **6**-AuNPs) is associated with their increased singlet oxygen quantum yields compared to the TiPc complexes alone, Table 2. Thus the presence of AuNPs results in the increase in singlet oxygen, which then results in a more efficient phototransformation of cyclohexene.

The percentage conversion variations are shown in Fig. 5 over 180 min. The first 30 min shows a drastic increase in the percentage conversion for all the complexes. This is followed by a slow conversion process until the reaction was stopped at 180 min.

$$MPc \longrightarrow {}^1MPc^* \longrightarrow {}^3MPc^* \quad (5)$$

$${}^3MPc^* + {}^3O_2 \longrightarrow {}^1O_2 \quad (6)$$

$${}^1O_2 + MPc \longrightarrow \text{Oxidation Products (phthalimide)} \quad (7)$$

Scheme 2. *Type II mechanism*. Here MPc is the metallophthalocyanine, ISC is intersystem crossing and Subs is the substrate. $^3O_2$ represents $O_2(^3\Sigma_g)$ and $^1O_2$ represents $O_2(^1\Delta_g)$.

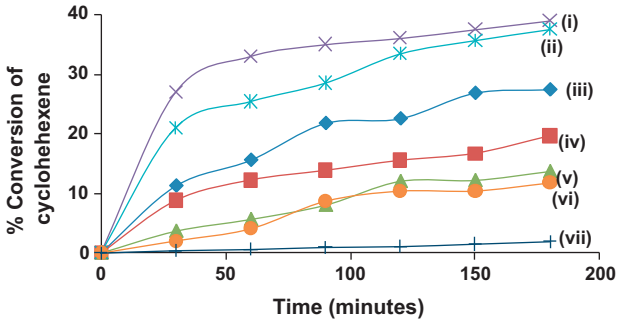

Fig. 5. Plots of percentage conversion of cyclohexene over a period of 180 min, where (i) is **5**-AuNPs, (ii) **6**-AuNPs, (iii) **5,** (iv) **6**, (v) **7**, (vi) **7**-AuNPs and (vii) **5** in the presence of DABCO in toluene. [**5**] = 3.1×10^{-5} mol L^{-1} or [**6**] = 4.30×10^{-5} mol L^{-1}, or [**7**] = 4.82×10^{-5} mol L^{-1}, [cyclohexene] = 4.06×10^{-2}. DABCO = 0.0029 g mL^{-1}.

The conjugated complexes, **5**-AuNPs and **6**-AuNPs, gave the highest percentage conversion values followed by complex **5**. **7**-AuNP shows the lowest conversion rate at all times corresponding to the low Φ_Δ value. In the presence of a singlet oxygen scavenger, DABCO [Fig. 6 (vii)], the percentage conversion of complex **5** was very minute (2% after 180 min). The low percentage conversion values in the presence of DABCO suggest that singlet oxygen is the most active species in the photo-transformation of cyclohexene. On the other hand, the slight conversion of cyclohexene in the presence of DABCO implies that it is not only singlet oxygen that is involved; there is a likelihood of involvement of other reactive oxygen species. To prove that other radicals were involved, photolysis of cyclohexene in the presence of benzoquinone (free radical scavenger) was carried out. A decrease of less than 1% was observed illustrating that free radicals were involved, to a very small extend.

The phthalocyanines employed in this work experienced photobleaching during catalysis as illustrated in Fig. 6a–d. The TaPc complex (**7**), Fig. 5a, and complex **7**-AuNPs (figure not shown) did not experience extreme photobleaching compared to complexes **5** and **6** and their AuNPs conjugates. Complex **5**, Fig. 6b, experienced less photobleaching (~50%) compared to its corresponding AuNP conjugate (**5**-AuNPs) at 72%, Fig. 6c. These observations further reiterate the involvement singlet oxygen in the photo-transformation of cyclohexene and the photodegradation of MPcs since increased singlet oxygen quantum yield values were observed on introducing AuNPs for complexes **5** and **6**. Similarly, complex **6**-AuNPs, Fig. 6d, showed drastic photobleaching of up to ~80%. In the presence of DABCO (figure not shown) photobleaching of the MPc complexes was minimal again illustrating the involvement of singlet oxygen in the photo-oxidation reactions. It is important to note that comparing Figs. 4a and 6b–d, the latter shows faster degradation of the phthalocyanine derivatives due to the higher light intensity used for phototransformation of cyclohexene.

The product yields as well as percentage selectivity values are presented in Table 3 after 180 min of irradiation. The values were higher than reported in literature [9,10]. The product yields ranged from 1.7% to 13.7%. The main product for **5** and **5**-AuNP with the largest Φ_Δ values is cyclohexene oxide. While for **7** and **7**-AuNP, with very low Φ_Δ values, the main product is cyclohexenediol. This suggests that the amount of singlet oxygen present, determines the yield of the products formed.

Alcohol is one of the desired products derived from oxidation of alkenes in the petrochemical industry. The product yields for 2-cyclohexene-1-ol were 6.6% and 9.1%, for complexes **5** and **6**, respectively. For complex **7**, a lower value of 5.9% was obtained.

The percentage selectivity values in Table 3 are higher for cyclohexene oxide compared to the other products when using complexes **5** and **6** and their corresponding AuNPs conjugates. The percentage selectivity values increased from 28.4% and 32.4% for **5** and **6**, respectively, to 40.3% and 36.9% for **5**-AuNPs and **6**-AuNPs, respectively. The highest selectivity for complex **7** was for 1,2-cyclohexanediol. The values were 24.5% for **7** and 17.6% for **7**-AuNP.

Fig. 7a–c shows the percentage selectivity values over a period of 180 min for complexes **6**, **6**-AuNPs and **7**-AuNPs, respectively. Fig. 7a–c shows a marked increase in % selectivity values for the first 30 min, followed by slowing down until photolysis was stopped at 180 min. For, complexes **5**, **5**-AuNp, **6** and **6**-AuNP (only **6** and **6**-AuNP shown in Fig. 7a and b, respectively), the selectivity was towards cyclohexene-1-one until after about 120 min, when the selectivity for cyclohexene oxide became more prominent. On the other hand, for **7** and **7**-AuNP, the lowest selectivity is for cyclohexenen-1-one for the entire 180 min, and the selectivity for cyclohexenediol was the highest for most of the time for **7** and **7**-

Table 3
Percentage selectivity values for cyclohexene photocatalytic products. Photolysis time = 180 min.

MPc	Product	% selectivity[a]	Product yields (%)[b]
5	Cyclohexene oxide	28.4	5.7
	2-Cyclohexen-1-ol	22.9	6.6
	2-Cyclohexene-1-one	17.0	5.1
	1,2-Cyclohexanediol	4.3	1.7
6	Cyclohexene oxide	32.4	6.8
	2-Cyclohexen-1-ol	24.4	9.1
	2-Cyclohexene-1-one	26.2	11.8
	1,2-Cyclohexanediol	2.8	13.7
7	Cyclohexene oxide	12.3	5.8
	2-Cyclohexen-1-ol	11.6	5.9
	2-Cyclohexene-1-one	9.7	5.6
	1,2-Cyclohexanediol	24.5	9.6
5-AuNP	Cyclohexene oxide	40.3	12.3
	2-Cyclohexen-1-ol	26.3	6.9
	2-Cyclohexene-1-one	26.8	7.1
	1,2-Cyclohexanediol	7.2	2.6
6-AuNP	Cyclohexene oxide	36.9	7.3
	2-Cyclohexen-1-ol	28.9	5.6
	2-Cyclohexene-1-one	29.1	13.1
	1,2-Cyclohexanediol	8.6	2.3
7-AuNP	Cyclohexene oxide	12.9	4.2
	2-Cyclohexen-1-ol	8.6	3.1
	2-Cyclohexene-1-one	7.2	3.3
	1,2-Cyclohexanediol	17.6	9.6

[a] % selectivity = $\text{epoxide}_{\text{obtained}}/[(1 - \text{cyclohexene}_{\text{initial}}) - (1 - \text{cyclohexene}_{\text{final}})]$.
[b] Based on the substrate cyclohexene.

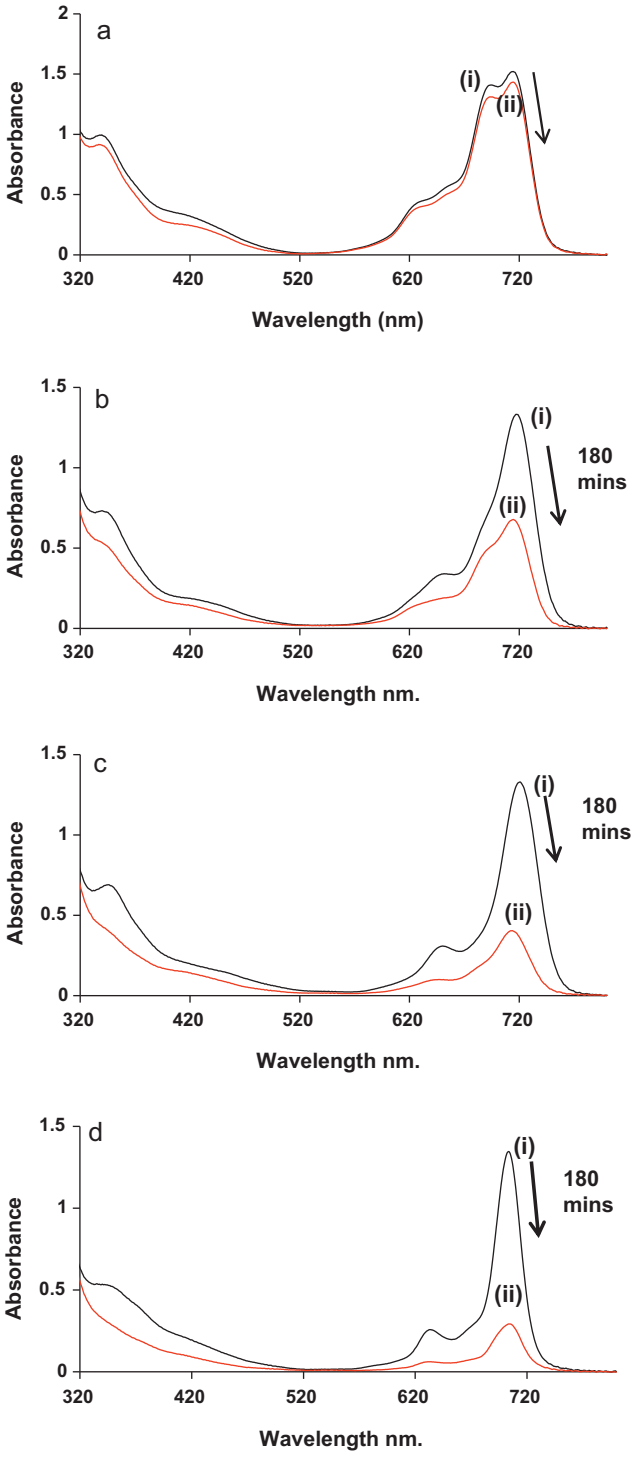

Fig. 6. Spectral changes observed for complex (a) **7**, (b) **5**, (c) **5**-AuNPs and (d) **6**-AuNPs during the photocatalytic transformation of cyclohexene. Irradiation over 180 min (i) before and (ii) after photolysis.

AuNPs. The selectivity for cyclohexene-diol was low for complexes **5** and **6** and their conjugates with AuNPs.

Two major pathways are suggested for the sensitisation reactions by phthalocyanines in literature. One involves the energy transfer from an electronically excited complex to ground state molecular oxygen that then yields singlet oxygen (Scheme 2) [3], Type II mechanism. The second mechanism involves the electron transfer from the excited complex to ground state molecular oxygen or reacting substrates thereby generating radicals such as

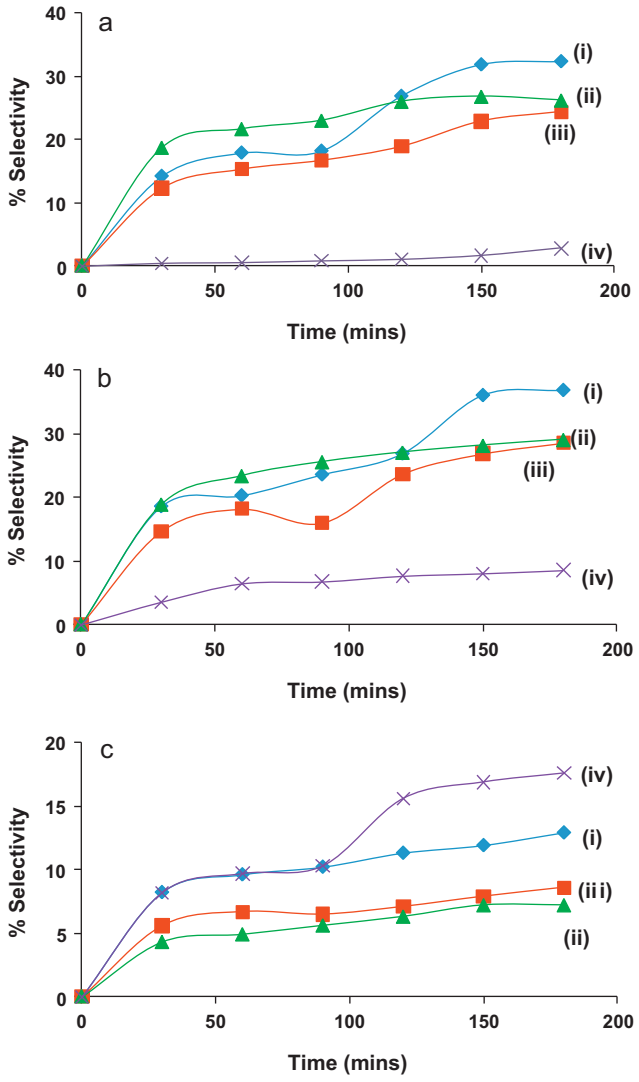

Fig. 7. Percentage selectivity plots of cyclohexene products in toluene using complex (a) **6**, (b) **6**-AuNPs and (c) **7**-AuNPs; where (i) cyclohexene oxide, (ii) cyclohenene-1-one, (iii) 2-cyclohexen-1-ol and (iv) 1,2-cyclohexenediol [**6**] = 4.30×10^{-5} mol L^{-1}.

superoxide radicals, Type I mechanism. As stated above, the % conversion of cyclohexene was slowed down in the presence of DABCO, Fig. 5. This, thus, implicates singlet oxygen as a major phototransformer in photocatalytic oxidation, as shown in the proposed mechanism in Scheme 3.

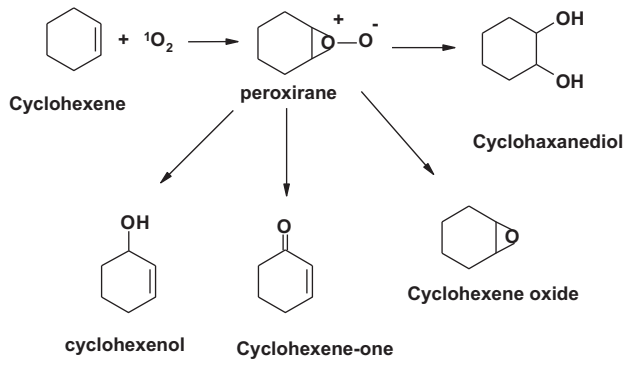

Scheme 3. Proposed mechanism for the formation of the photo-oxidation products.

4. Conclusion

The synthesis of TiPc (**5** and **6**) and TaPc (**7**) complexes was achieved. The complexes showed solubility in most common organic solvents such toluene and chloroform. The photochemical parameters, i.e. the singlet oxygen and photodegradation quantum yields were determined for complexes **5**–**7** as well as their corresponding AuNPs conjugates. The complexes were very stable, within the normal stability range for phthalocyanines. The singlet oxygen production was improved significantly by the presence of AuNPs, except for TaPc, **7**, and **7**-AuNPs. Photocatalytic oxidation of cyclohexene was carried out effectively where the percentage conversion of cyclohexene was significantly improved by the presence of gold nanoparticles. The products obtained are: cyclohexene oxide, cyclohexenol, cyclohexenone and cyclohexanediol. Future work will involve changing the size of the AuNPs and determining the effects of the change in size on product yield and selectivity.

Acknowledgements

This work was supported by the Department of Science and Technology (DST) and National Research Foundation (NRF) of South Africa through DST/NRF South African Research Chairs Initiative for Professor of Medicinal Chemistry and Nanotechnology and Rhodes University.

References

[1] F.H. Moser, A.L. Thomas, Phthalocyanines Compounds, Reinhold Publishers, New York, 1963.
[2] M.A. Zanjanchi, A. Ebrahimian, M. Arvand, J. Hazard. Mater. 175 (2010) 992.
[3] R. Bonnett, Chemical Aspects of Photodynamic Therapy, Gordon and Breach Science Publishers, Germany, 2000.
[4] I.A. Levitsky, W.B. Euler, N. Tokranova, B. Xu, J. Castracene, Appl. Phys. Lett. 85 (2004) 6245.
[5] A.B. Sorokin, S. Mangematin, C. Pergrale, J. Mol. Catal. A: Chem. 182–183 (2002) 267.
[6] R. Hage, A. Lienke, J. Mol. Catal. A: Chem. 251 (2006) 150–158.
[7] N. Nensala, T. Nyokong, J. Mol. Catal. A 164 (2000) 69.
[8] K. Lang, J. Mosinger, D. Wagnerova, Chem. Listy 99 (2005) 211.
[9] X. Xue, Y. Xu, J. Mol. Catal. A 276 (2007) 80.
[10] N. Sehlotho, T. Nyokong, J. Mol. Catal. A: Chem. 209 (2004) 51.
[11] P. Tau, T. Nyokong, J. Mol. Catal. A: Chem. 52 (2007) 3641.
[12] P. D'Ambrosio, L. Tonucci, N. D'Alessandro, A. Morvillo, S. Sortino, M. Bressan, Eur. J. Inorg. Chem. (2011) 503.
[13] T. Nyokong, E. Antunes, in: K.M. Kadish, K.M. Smith, R. Guilard (Eds.), The Handbook of Porphyrin Science, vol. 7, Academic Press/World Scientific, New York/Singapore, 2010, pp. 247–349 (chapter 34).
[14] S. Eustis, M.A. El-Sayed, Chem. Soc. Rev. 35 (2006) 209.
[15] S. Yamad, T. Tasaki, T. Akiyama, N. Terasaki, S. Nitahara, Thin Solid Films 70 (2003) 438.
[16] S. Fukuzumi, Y. Endo, Y. Kashiwagi, Y. Araki, O. Ito, H. Imahori, J. Phys. Chem. B 107 (2003) 11979.
[17] S. Link, M.A. El-Sayed, Annu. Rev. Phys. Chem. 54 (2003) 331.
[18] C.F. Bohrem, D.R. Huffman, Absorption and Scattering of light by Small Particles, Wiley, New York, 1983.
[19] P. Mulvaney, Langmuir 12 (1996) 788.
[20] V.P. Chauke, E. Antunes, W. Chidawanyika, T. Nyokong, J. Mol. Cat. A: Chem 335 (2011) 121.
[21] P. Tau, T. Nyokong, Dalton Trans. (2006) 4482–4490.
[22] P. Gregory, J. Porphyr. Phthalocya. 4 (2000) 432–437.
[23] M. Brust, M. Walker, D. Bethell, D.J. Schiffrin, R. Whyman, J. Chem. Soc., Chem. Commun. (1994) 801.
[24] A. Kotiaho, R. Lahtinen, A. Efimov, H.-K. Metsberg, E. Sariola, H. Lehtivuori, N.V. Tkachenko, H. Lemmetyinen, J. Phys. Chem. C 114 (2010) 162.
[25] T. Nyokong, Coord. Chem. Rev. 251 (2007) 1707.
[26] G. Schnurpfeil, A. Sobbi, W. Spiller, H. Kliesch, D. Wöhrle, J. Porphyr. Phthalocya. 1 (1997) 159.
[27] P. Kubát, J. Mosinger, J. Photochem. Photobiol. A: Chem. 96 (1996) 93.
[28] S.M. Bishop, A. Beeby, A.W. Parker, M.S.C. Foley, D. Phillips, J. Photochem. Photobiol. A: Chem. 90 (1995) 39.
[29] N. Sehlotho, M. Durmus, V. Ahsen, T. Nyokong, Inorg. Chem. Commun. 11 (2008) 479.
[30] V.P. Chauke, W. Chidawanyika, T. Nyokong, Electroanalysis 23 (2011) 487.
[31] H. Isago, T. Nyokong, J. Porphyr. Phthalocya. 8 (2004) 1083.
[32] T. Fukuda, T. Ishiguro, N. Kobayashi, Tetrahedron Lett. 46 (2005) 2907.
[33] S. Perun, J. Tatchen, C.M. Marian, Chem. Phys. Chem. 9 (2008) 282.
[34] S. Maree, T. Nyokong, J. Porphyr. Phthalocya. 5 (2001) 2985.